MAGNETOHYDRODYNAMICS Vol. 37 (2001), No. 1-2, pp. 135–142

NATURAL CONVECTION IN RECTANGULAR ENCLOSURES OF ARBITRARY ORIENTATION WITH MAGNETIC FIELD VERTICAL – PROBLEM REVISITED

M. D. Cowley, D. J. MacLean, T. Alboussière

Cambridge University Engineering Department

This paper carries the investigation of natural convection in tilted containers a stage beyond the asymptotic analysis of [1], with the full equations being solved numerically by the commercial code CFX. Comparisons are made with the asymptotic solutions and good agreement is found at low values of $\mathrm{Ra}/\mathrm{Ha}^2$. On the other hand, the prediction for high values, that there is a core of stationary fluid in a uniform vertical temperature gradient, is approached only slowly as $\mathrm{Ra}/\mathrm{Ha}^2$ is increased. The behaviour can be explained by extending the asymptotic analysis to the next order of approximation.

Introduction. It was suggested in a previous paper [1] that tilted containers provide an interesting geometry for testing general ideas on natural convection in the presence of a vertical magnetic field. Particularly simple asymptotic solutions could be developed for the cases of (i) negligible advection of temperature and (ii) advection strong enough to lead to a core in which the temperature distribution is stably stratified. With neglect of inertia and with viscous effects confined to thin layers ($\mathrm{Ha} \gg 1$), the controlling parameter was found to be $\mathrm{Ra}/\mathrm{Ha}^2$, where Ra is the Rayleigh number and Ha the Hartmann number, the parameter being much less than unity for case (i) and much greater than unity for case (ii). The development by one of us (DJM) of a computational scheme for the numerical simulation of natural-convection problems in MHD has now provided an opportunity to check the relevance of the asymptotic analysis.

1. Recapitulation. Definitions and details of the derivation of the governing equations have been given in the previous paper [1], but the most important points are as follows. The geometry of the two-dimensional container is illustrated in Fig. 1. Two plane walls are taken to be thermally insulating and two thermally conducting with a boundary condition of uniform heat flux $\dot{q}_\mathrm{w}$. In contrast to [1] the cross-section of the container is square and the full length of each side d is the scale used for reduction of the equations to non-dimensional form. The reduced equations expressing balance of rotational forces and of energy are

$$\underset{\text{inertia}}{\frac{\mathrm{Ra}}{\mathrm{Pr}\,\mathrm{Ha}^2}\frac{\partial(\Psi,\Omega)}{\partial(Z,X)}} = \underset{\text{e.m. force}}{-\frac{\partial^2\Psi}{\partial Z^2}} \underset{\text{buoyancy}}{-\frac{\partial\theta}{\partial X}} + \underset{\text{viscous}}{\frac{1}{\mathrm{Ha}^2}\nabla^2\Omega}, \tag{1}$$

$$\frac{\mathrm{Ra}}{\mathrm{Ha}^2}\frac{\partial(\Psi,\theta)}{\partial(Z,X)} = \nabla^2\theta, \tag{2}$$

where Ψ, Ω and θ are non-dimensional stream function, vorticity and temperature respectively, Ψ being such that $\partial\Psi/\partial Z$ is the non-dimensional velocity in the X-

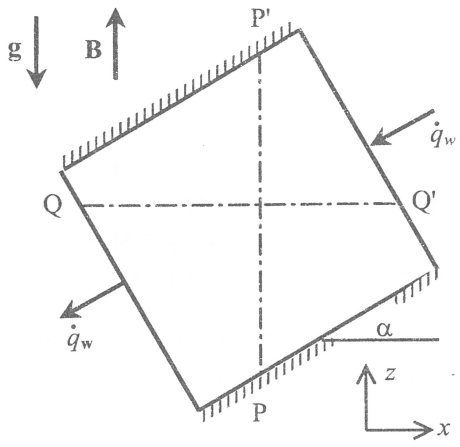

Fig. 1. Tilted container geometry.

direction. The link between Ψ and Ω is given by

$$\Omega = \nabla^2 \Psi. \tag{3}$$

The geometry of the flow and the direction of the magnetic field imply zero electric field, so that current (direction perpendicular to the flow plane) is proportional to the velocity component in the X-direction and the e.m. force then takes the form shown in equation (1).

The non-dimensional parameters of equation (1) are the Rayleigh number, Prandtl number and Hartmann number, given by

$$\mathrm{Ra} = \frac{\rho^2 c \beta g \dot{q}_w d^4}{\lambda \mu}, \quad \mathrm{Pr} = \frac{c\mu}{\lambda}, \quad \mathrm{Ha} = Bd\sqrt{\frac{\sigma}{\mu}}, \tag{4}$$

wherein $\dot{q}_w d/\lambda$ is the effective temperature scale.

The boundary conditions are

$$\begin{gathered} \Psi = 0, \ \partial\Psi/\partial n = 0 \quad \text{at all walls;} \\ \partial\theta/\partial n = \pm 1 \quad \text{at walls with heat flux to/from the fluid;} \\ \partial\theta/\partial n = 0 \quad \text{at thermally insulating walls,} \end{gathered} \tag{5}$$

where $\partial\theta/\partial n$ is the outward normal gradient.

1.1. Negligible advection of temperature. When $\mathrm{Ra}/\mathrm{Ha}^2 \to 0$, heat flow through the enclosure is governed by conduction only (see Eq. (2)), with isotherms parallel to the diabatic walls and temperature gradient uniform. As discussed in [1], if there is a core flow which can be treated as inviscid and inertialess ($\mathrm{Ha} \gg 1$), equation (1) reduces to

$$\partial^2\Psi/\partial Z^2 = -\partial\theta/\partial X = \text{const},$$

so that in the core $\Psi = \Psi_c$ has a parabolic distribution with Z along field lines like PP′ on Fig. 1, being zero at the the edges of the core. In a region where field lines cut two parallel walls, the streamlines will be parallel to those walls and the flow is one of uniform shear. In regions where field lines cut walls which

are perpendicular to each other streamlines are rectangular hyperbolae [1]. It was suggested in [1] that, where the two types of flow meet, parallel layers of thickness $O(\mathrm{Ha}^{-1/2})$ occur.

1.2. Strong advection of temperature. The proposal in [1] for asymptotic behaviour at high values of $\mathrm{Ra}/\mathrm{Ha}^2$ was for a motionless core where the temperature gradient is vertical and uniform. Boundary layers are formed on the walls in order to adjust temperature gradients so as to satisfy the conditions on $\partial\theta/\partial n$ imposed by equations (5). Interestingly enough, it is not necessary to solve the equations governing the layers in order to determine the net flow in them and the temperature gradient in the core. If we consider a horizontal line such as QQ′ on Fig. 1, there can be no net flow across it and at the limit the temperature on it is constant. Therefore there is zero net thermal energy flux by convection. Energy flux by conduction across QQ′ must equate to the net flux supplied by $\dot{q}_\mathrm{w}$ on one side of QQ′. This leads to $\partial\theta/\partial Z = \sin\alpha$, so that in the core $\theta = \theta_\mathrm{c}$ has a uniform Z–wise gradient. Across a vertical line such as PP′, there is no conduction because the temperature gradient is vertical. However, there is, now a temperature difference between the ends of the line and consequentially a flux of energy by convection. Equating this to the net wall flux on either side leads to a core value $\Psi_\mathrm{c} = (\mathrm{Ha}^2/\mathrm{Ra})\cot\alpha$.

2. Numerical simulation. Solutions to Eqs (1), (2) and (3) with inertia and viscous terms retained have been found using the commercial finite-volume package CFX with appropriate modification to include the electromagnetic-force term. The grid used had 320 by 320 cells and a geometric progression of common ratio 1.02 concentrated the mesh close to the walls. The chosen grid ensured that there were 7 cells or more within the thickness of the Hartmann layers. A sample of the results is shown in Fig. 2 for containers tilted at $\alpha = 30°$ to the horizontal, with $\mathrm{Ha} = 1000$ and $\mathrm{Pr} = 1$. Although the latter is not a reasonable value for liquid metals, it becomes computationally very time consuming to solve for a parameter range where Pr is small and inertia still weak.

2.1. Weak advection of temperature, $\mathrm{Ra}/\mathrm{Ha}^2 = 10^{-2}$. The top row of plots in Fig. 2 refers to conditions such that temperature advection is weak, the isotherms in 2*c* being very nearly parallel to the diabatic walls. The streamlines of 2*a* conform with the asymptotic expectation of a uniform shear flow between the adiabatic walls and turn-round regions where streamlines are rectangular hyperbolae. However, it is noticeable that where the two types of flow meet there is a smooth rounded transition of the streamline direction.

If the stream function Ψ_c of the asymptotic core flow as $\mathrm{Ra}/\mathrm{Ha}^2 \to 0$ is subtracted from the numerical solution (Fig. 2*b*, the presence of parallel layers of thickness $O(\mathrm{Ha}^{-1/2})$ becomes apparent.

2.2. Moderate advection of temperature, $\mathrm{Ra}/\mathrm{Ha}^2 = 1$. The next row of plots refers to conditions where it might be expected that thermal convection is becoming comparable in importance to conduction. Fig. 2*f* shows that the isotherms are shifted, but not to a great extent. Similarly, the streamline plot of Fig. 2*d* looks hardly different from that of Fig. 2*a*, but close inspection shows that the streamlines have been shifted outwards (values of streamfunction on the lines are the same as those in 2*a*). Subtraction of the asymptotic streamfunction Ψ_c as $\mathrm{Ra}/\mathrm{Ha}^2 \to 0$ from the numerical solution results in Fig. 2*e*, where $\Psi - \Psi_\mathrm{c}$ is typically 0.1 times Ψ.

[1] The expression for Ψ given in [1] is incorrect. It should read $\Psi_\mathrm{c} = -1/2\cos(Z - X\tan\alpha)(Z + X\cot\alpha)$.

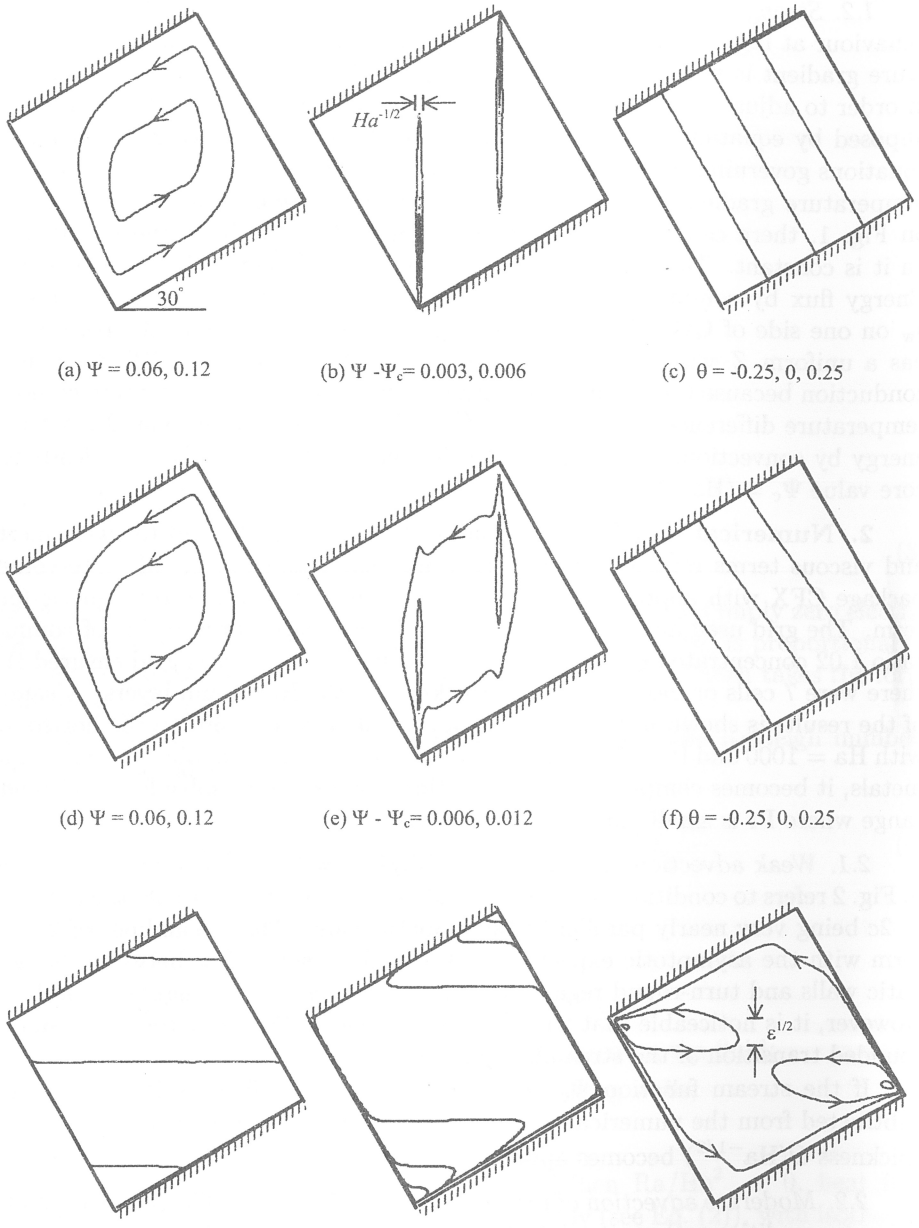

(a) $\Psi = 0.06, 0.12$ (b) $\Psi - \Psi_c = 0.003, 0.006$ (c) $\theta = -0.25, 0, 0.25$

(d) $\Psi = 0.06, 0.12$ (e) $\Psi - \Psi_c = 0.006, 0.012$ (f) $\theta = -0.25, 0, 0.25$

(g) $\theta = -0.25, 0, 0.25$ (h) $\theta - \theta_{0c} = \pm 0.005, \pm 0.015, \pm 0.025$ (i) $\Psi Ra/Ha^2 = 2.0, 1.75, 1.5$

Fig. 2. Streamlines and isotherms for $\mathrm{Ra/Ha^2} = 10^{-2}$ (a, b, c), 1 (d, e, f) and 10^4 (e, h, i). $\mathrm{Ha} = 10^3$ for all cases. Ψ_c is the asymptotic value in the core as $\mathrm{Ra/Ha^2} \to 0$; θ_{0c} is the asymptotic value in the core as $\mathrm{Ra/Ha^2} \to \infty$.

2.3. Strong advection of temperature, $\mathrm{Ra/Ha^2} = 10^4$. The strong advection limit is not approached closely until $\mathrm{Ra/Ha^2}$ is of order 10^4. However, even at 10^4 subtraction of the asymptotic result for θ_c as $\mathrm{Ra/Ha^2} \to \infty$, i.e. $\partial\theta_c/\partial Z = \sin\alpha$ (see 1.2), from the numerical solution (Fig. 2*h*) shows that there is a significant departure from the expected uniformity of core temperature gradient. The streamlines of 2*i* present even more of a challenge to the asymptotic theory, which predicts a motionless core with $\Psi_c = 3^{1/2}(\mathrm{Ha^2/Ra})$ for $\alpha = 30°$, whereas the numerical solution has Ψ varying over the core region from approximately 1.4 to 2.0 times $(\mathrm{Ha^2/Ra})$.

3. Further analysis for $\mathrm{Ra/Ha^2} \gg 1$.

3.1. Temperature field. According to [1] boundary layers at the walls when $\mathrm{Ra/Ha^2}$ is large have thickness $O(\varepsilon)$, where $\varepsilon = \mathrm{Ha/Ra^{1/2}}$. If it is supposed that solutions for θ can be expanded as power series in ε,

$$\theta = \theta_0 + \varepsilon\theta_1 + \varepsilon^2\theta_2 \cdots \tag{6}$$

θ_0 is the leading-order solution, with $\mathrm{d}\theta_0/\mathrm{d}Z = \sin\alpha$ (see 1.2) in both boundary layers and core. Although the next term in the series is of order ε, its gradient in a boundary layer is of order unity because the length scale is of order ε there. Thus the boundary condition at the wall on heat flux (see Eq. (5)) can be met. Consistent with the series (6) for θ is a series for Ψ of the form

$$\Psi = \varepsilon^2\Psi_2 + \varepsilon^3\Psi_3 \cdots, \tag{7}$$

where $\varepsilon^2\Psi_2$ takes the leading-order value $(\mathrm{Ha^2/Ra})\cot\alpha$ in the core (see 1.2.), but, whereas Ψ_2 is constant there, it varies in the boundary layers, being zero at the walls.

Solutions of the equations for θ_1 and Ψ_2 have been given in essence by [1] for the case of $\varepsilon \gg \mathrm{Ha^{-1}}$, when viscous action is confined to thin Hartmann layers on the walls, and in the main body of the boundary layers θ_1 and Ψ_2 have exponential form

$$\theta_1 = \theta_{1c} + \chi\cos\alpha\,(\mathrm{d}\theta_0/\mathrm{d}Z)^{1/2}\exp(kn/\varepsilon), \tag{8}$$

$$\Psi_2 = \cot\alpha\Big\{1 - \exp(kn/\varepsilon)\Big\}, \tag{9}$$

where on *diabatic* walls $\chi = -1$ and $k = \cot\alpha\,(\mathrm{d}\theta_0/\mathrm{d}Z)^{1/2}$, and on *adiabatic* walls $\chi = \cot^2\alpha$ and $k = \tan\alpha\,(\mathrm{d}\theta_0/\mathrm{d}Z)^{1/2}$; n is the outward normal co-ordinate and θ_{1c} the core value of θ_1, taken to be a function of Z only.

To determine θ_{1c} a similar method to that of 1.1. is adopted. Consider the horizontal line QQ′ in the sketch of Fig. 3. In the core the line co-incides with a particular isotherm $\theta_{0c} + \varepsilon\theta_{1c}$, but near the diabatic walls it departs from that isotherm. Arrows on the sketch indicate the direction of flow in the boundary layers associated with Ψ_2. It will be seen that on the horizontal θ is less than the core temperature where the flow is downward and greater where the flow is upward. In contrast to the solution taken to leading-order only there is now a net upward flux of thermal energy by convection across QQ′. The amount associated with each layer is given by integration across it as

$$\varepsilon\int_{n=0}^{-\infty}(\theta_1 - \theta_{1c})\,\mathrm{d}\Psi_2.$$

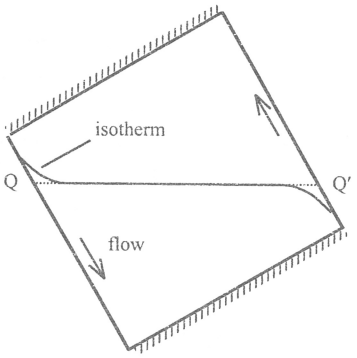

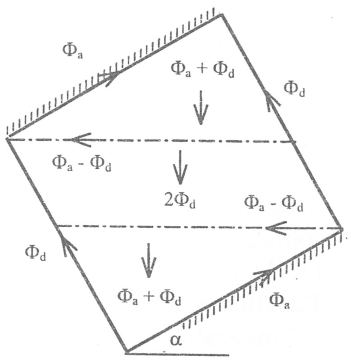

Fig. 3. Isotherm shape for $\mathrm{Ra}/\mathrm{Ha}^2 \gg 1$.

Fig. 4. Energy flux function for $O(\varepsilon)$ contribution ($\alpha < 45°$).

However, the above integral is not the only correction to the energy flux. Conduction is affected by the temperature gradient associated with $\theta_1 - \theta_{1c}$ in each layer and with θ_{1c} over the full length of QQ′. Let the contribution to energy flux (convection and conduction) for each diabatic-wall layer be $\varepsilon\Phi_d$, where

$$\varepsilon\Phi_d = \varepsilon \int_{n=0}^{-\infty} (\theta_1 - \theta_{1c})\, d\Psi_2 + \varepsilon \int_{n=0}^{-\infty} (\partial\,(\theta_1 - \theta_{1c})\,/\partial Z)\, dX =$$

$$= \frac{1}{2}\varepsilon \sin\alpha(\cot^2\alpha - 2)\left(\frac{d\theta_0}{dZ}\right)^{1/2}, \tag{10}$$

the integrals being evaluated using expressions (8) and (9). In a similar fashion the contribution from each adiabatic-wall layer $\varepsilon\Phi_a$ is found to be

$$\varepsilon\Phi_a = \frac{3}{2}\varepsilon \sin\alpha \cot^2\alpha \left(\frac{d\theta_0}{dZ}\right)^{1/2}. \tag{11}$$

These energy fluxes for $\alpha < 45°$ are illustrated in Fig. 4, which also shows that, to achieve energy balance, there must be consequent fluxes, downward through the core and feeds between the core and the layers at the corners of the container. The fluxes differ slightly for $\alpha > 45°$, but the principles are the same as for $\alpha < 45°$.

Within the lozenge shaped region at the centre of the container (bounded by two horizontals and two parallel walls) the energy flux in the core can be uniformly distributed and can therefore be driven by conduction due to a uniform gradient $d\theta_{1c}/dZ$. On the other hand, within the top and bottom triangular regions, the length of a horizontal line between walls (one diabatic, the other adiabatic) varies linearly with distance from the top and bottom corners respectively. To maintain a constant heat flux through each region $d\theta_{1c}/dZ$ must vary inversely with distance from top or bottom corner, as appropriate, i.e. θ_{1c} must vary logarithmically with Z, becoming singular at the top and bottom corners, where the present approximations will break down. A further complication arises from $d\theta_{1c}/dZ$ being non-uniform. In order to satisfy the thermal energy equation (2) in the core, there must be a convective term to balance $d^2\theta_{1c}/dZ^2$. However, this can be achieved with an order ε^3 flow interacting with the leading-order temperature field and calculations based on an order ε^2 flow field are not invalidated.

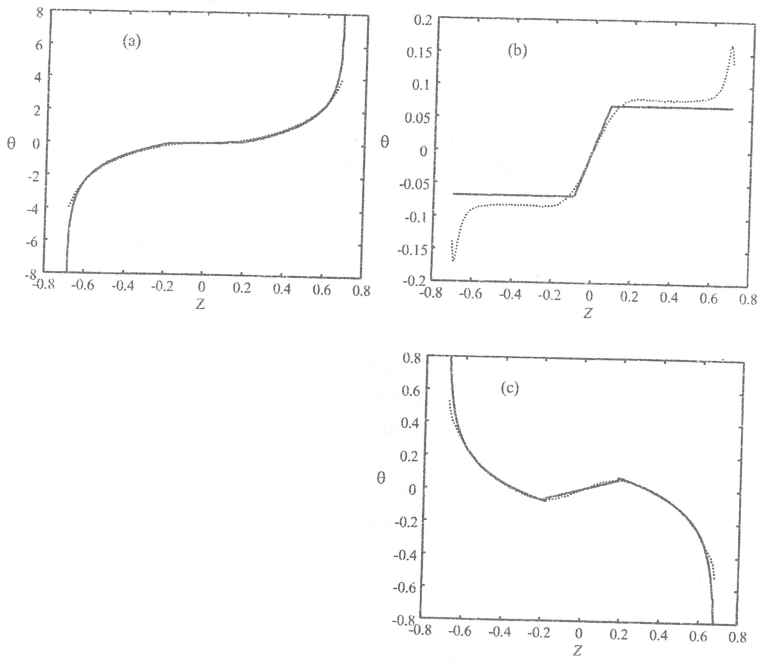

Fig. 5. Comparison of $O(\varepsilon)$ corrections to leading order predictions of temperature distributions in the core for the θ_{1c} (solid curve) and $(\theta - \theta_{0c})/\varepsilon$ (dashed curve). $\alpha = 30°$ (a), 52.2° (b), 60° (c). $\mathrm{Ha} = 10^3$, $\mathrm{Ra} = 10^{10}$ in all cases.

In Fig. 5 analytical results for θ_{1c} are plotted against the Z co-ordinate, the origin being at the centre point of the container and the results are compared with predictions for $(\theta - \theta_{0c})/\varepsilon$. θ is evaluated from the numerical simulation on a straight line between the top and bottom corners and θ_{0c} from the asymptotic results. The origin for the Z co-ordinate is the centre point of the container. For Fig. 5*a* the tilt angle $\alpha = 30°$ is the same as for Fig. 2*h* and it is seen that the departure of the numerical solution from the leading-order asymptotic result is almost entirely associated with the $O(\varepsilon)$ correction. A feature of this case is that the contribution of $\varepsilon\theta_{1c}$ to the temperature gradient is comparatively small in the central lozenge. Reference to Fig. 4*d* shows that additional flux in the lozenge will be zero when Φ_d is zero and according to equation (10) this occurs when $\cot^2\alpha = 2$, i.e. $\alpha = 35.3°$, which is not very much greater than the tilt angle of Fig. 5*a*.

Of particular interest is the case where the angle of tilt is such that $\Phi_d = -\Phi_a$. According to equations (10) and (11), this happens when $\cot^2\alpha - 2 = -3\cot^3\alpha$, i.e. when $\alpha = 52.2°$. At this angle of tilt there will be no $O(\varepsilon)$ flux in the triangular regions and θ_{1c} will be constant there (see Fig. 5*b*).

When α is greater than 52.2°, Φ_d is less than Φ_a and the direction of the $O(\varepsilon)$ fluxes in the triangular regions reverses. In contrast to cases where α is less than 52.2° and the $O(\varepsilon)$ temperature gradient reinforces the leading-order gradient, the $O(\varepsilon)$ contribution now acts in opposition to $\mathrm{d}\theta_{0c}/\mathrm{d}Z$. This behaviour is illustrated in Fig. 5*c* for $\alpha = 60°$.

3.2. The flow field. Fig. 4 shows that there is another flux-balancing requirement with $\varepsilon(\Phi_a - \Phi_d)$ being fed into the core from the right-hand corner and the same flux into the left-hand corner. The plot of streamlines in figure 2*j* provides

the clue to the mechanism for this flux. If there can be an effective flow doublet at each corner with velocity to the left where the leading-order temperatures are relatively high and velocity to the right where they are relatively low, there will be a net flux of thermal energy to the left. It is easily verified that a substantially horizontal layer can be formed with vertical length scale $O(\varepsilon^{1/2})$, while $\Psi = O(\varepsilon^{5/2})$ and $\theta = O(\varepsilon^{3/2})$. The implication is that the series (6) and (7) must be modified so as to include terms like $\varepsilon^{3/2}\theta_{3/2}$ and $\varepsilon^{5/2}\Psi_{5/2}$. With this scaling and with inertia and viscous action neglected, equations (1) and (2) may be re-cast as

$$\left(\frac{\partial^2}{\varepsilon\partial Z^2} \pm \left(\frac{\mathrm{d}\theta_0}{\mathrm{d}Z}\right)^{1/2} \frac{\partial}{\partial X}\right)\left(\theta_{3/2} \pm \left(\frac{\mathrm{d}\theta_0}{\mathrm{d}Z}\right)^{1/2} \Psi_{5/2}\right) = 0, \qquad (12)$$

i.e. a combination of two linear diffusion equations. Complexity of boundary conditions precludes a simple analytical solution to equation (12), although similarity solutions are easily found and provide some indication of behaviour. It may be shown that they relate to the horizontal layer which was derived in [1]. For present purposes the interesting points are first that the temperature levels do not formally invalidate the previous $O(\varepsilon)$ analysis for θ_{1c} and second the stream function differs from leading order by a factor $O(\varepsilon^{1/2})$, which is only 0.1 for the case shown in Fig. 2*i*. A signicant departure from the leading-order prediction, $\varepsilon^2\Psi_{2c}$, is not surprising.

Conclusions. The results of numerical simulation have confirmed the findings of asymptotic analysis for small and for large values of $\mathrm{Ra}/\mathrm{Ha}^2$.

REFERENCES

1. M. D. Cowley. Natural convection in rectangular enclosures of arbitrary orientation with magnetic field vertical. *Magnetohydrodynamics*, vol. 32 (1996), no. 3, pp. 390–398.

Received 01.02.2001